AGU100 ADVANCING EARTH AND SPACE SCIENCE

Water Resources Research

RESEARCH ARTICLE
10.1029/2017WR021378

New Hypothesis for the Final Equilibrium Stage of a River Levee Breach due to Overflow

Giovanni Michelazzo[1], **Hocine Oumeraci**[2], **and Enio Paris**[1]

[1]Department of Civil and Environmental Engineering, University of Florence, Florence, Italy, [2]Leichtweiss-Institute for Hydraulic Engineering and Water Resources, Division of Hydromechanics and Coastal Engineering, TU Braunschweig, Braunschweig, Germany

Key Points:
- A new hypothesis on the existence of an equilibrium stage in the breaching process of river levees is proposed and investigated
- The interaction between river dynamics and breach evolution determines the equilibrium condition of the breaching process
- Expeditious formulae are proposed for a first approximation of the breach flow and breach length at the equilibrium stage

Supporting Information:
- Supporting Information S1
- Data Set S1
- Data Set S2
- Data Set S3

Correspondence to:
G. Michelazzo,
ing.michelazzo@hotmail.com

Citation:
Michelazzo, G., Oumeraci, H., & Paris, E. (2018). New hypothesis for the final equilibrium stage of a river levee breach due to overflow. *Water Resources Research*, *54*, 4277–4293. https://doi.org/10.1029/2017WR021378

Received 24 JUN 2017
Accepted 28 MAY 2018
Accepted article online 6 JUN 2018
Published online 3 JUL 2018

Abstract Breaching of earthen embankments is a complex process that often results in disastrous inundations of the hinterland. The process has been studied during the last decades by means of physical and numerical modeling with particular reference to the dam case, while for river levees only few specific studies have been conducted. Moreover, the understanding and prediction of the breach final configuration are still scarce and not yet deeply addressed, despite their importance for mitigating flood risk in the protected areas. The paper attempts to examine the existence of a final equilibrium stage in the river-breach system under specified conditions based on a significant data set from new laboratory experiments. Using these data, together with those of previous studies, a new hypothesis for the final equilibrium of the river-breach system is proposed which is supported by new flow formulae and field data.

1. Introduction

Flooding from river levee breaches is a problem that often causes significant socioeconomic damages worldwide. Many countries have experienced such floods, among which Germany (Vorogushyn et al., 2010), Hungary (Nagy, 2006), Italy (Govi & Maraga, 2005; Viero et al., 2013), Bangladesh (Islam & Tsujimoto, 2011), China (Chen et al., 2012), Japan (Bhattarai et al., 2015), and United States (Sills et al., 2008) might be mentioned.

Earthen levees often represent the main structural system used for the defense against river flooding. Therefore, a great concern is put on their reliability, on their effectiveness, and on the emergency actions to limit the consequences of possible breaches. An important step to mitigate this type of flood risk is to understand the breaching process and to develop reliable tools to predict its development and its effect on the main parameters of the subsequent flooding (e.g., flow depth, velocity, discharge, and arrival time). Such knowledge might help (i) to warn at the earliest the population potentially affected by the inundation and (ii) to stop the process evolution through adequate emergency repair operations.

Several studies have been conducted on the initiation and development stages of the breaching process, yet many questions still remain unanswered. Most of the current knowledge focuses on breaching of dams, whereas levee breaches have received less attention despite the significant differences between the two processes (ASCE-American Society of Civil Engineers/EWRI-Environmental & Water Resources Institute Task Committee on Dam/Levee Breaching, 2011). Moreover, the dam breach models are hardly applicable to the river levee case apart from the very initial stages of the erosion process (Kakinuma & Shimizu, 2014).

The determination of the breach characteristics is highly complex, due to the diverse processes and nonlinear interactions between soil, water, and structure. The phenomenon is yet under investigation regarding the main breaching stages as well as the effect of single factors, such as the composition, compaction, and further characteristics of the levee material. This also includes the failure mechanisms mainly classified in (i) internal and external erosion induced by seepage and overflow, respectively, and (ii) mass instabilities (Construction Industry Research and Information Association, Ministry of Ecology, and United States Army Corps of Engineers, 2013).

Significant efforts have been deployed in the last decades in order to develop prediction models and formulae for the main breach characteristics, their temporal change, and their maximum or ultimate values. For instance, the overflow-induced breaching process has been divided into four main stages based on the degree of erosion of the embankment as depicted in Figure 1 (Viero et al., 2013):

1. Erosion is initiated by overflow at the landside slope.
2. The erosion progresses backward toward the embankment crest.

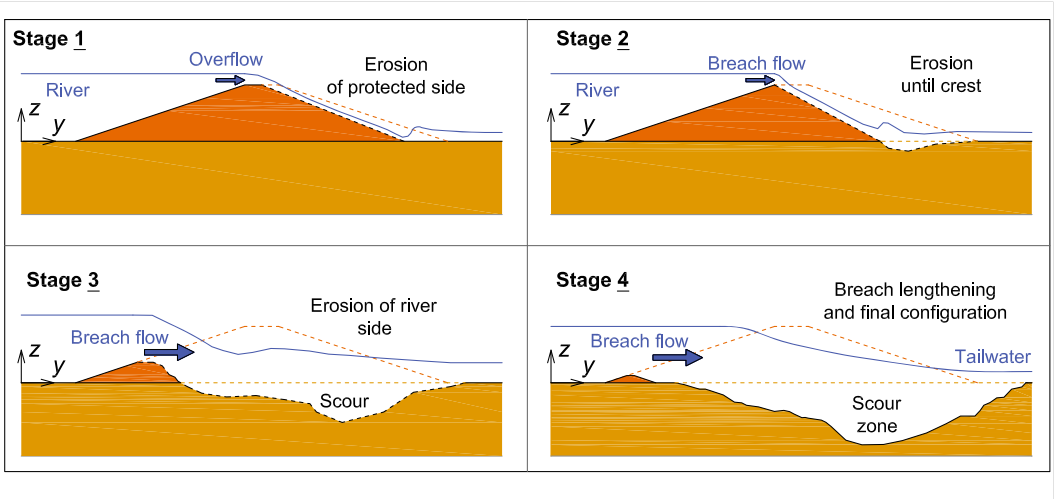

Figure 1. Stages of an overflow-induced breaching process.

3. The crest is completely eroded so that the flood source is directly connected with the protected side; the breaching process is accelerated and the breach lengthens quickly.
4. The breach lengthens until a final configuration is achieved.

The focus of the present research is the last, or the final, stage of the breaching process of earthen river levees (i.e., stage 4 of Figure 1); when the levee section is completely eroded, the breach lengthens according to the river flow action and a scour zone likely develops under the levee base. The breach and river variables (i.e., breach length and discharge, water level, downstream river discharge, and riverbed) change according to variations that are significantly smaller than those of the third breaching stage. Hence, from the experimental evidence, the existence of an asymptotic equilibrium can be postulated, where the breach keeps a stable configuration and the flow partition between the river and the breach is at equilibrium. However, an absolute steady equilibrium can hardly be achieved due to the feedbacks between the coupled hydromorphodynamic mechanisms governing the breach development and the changes in the river characteristics. Therefore, quasi steady states may develop, in which the breach and river variables change slowly toward asymptotic values according to variation rates that depend on the sediment transport and flow processes in both river and breach channels.

To the authors' knowledge, the first systematic laboratory study about river levee breaching was performed by Fujita and Tamura (1987), in which the breach evolution stages and the sediment erosion/deposition in the floodplain were analyzed. Kakinuma and Shimizu (2014) tested the effects of levee material, crest width, and inflow discharge on the breach development in large-scale experiments; a constant breach flow was measured during the final breaching stage.

Further laboratory and numerical experiments were conducted with a focus on the effects of grain size (Islam & Tsujimoto, 2015), riverbed elevation, material and slope (Bhattarai et al., 2015), and inflow-downstream conditions (Rifai et al., 2017) on the levee breach development. However, no systematic study on the final breaching stage is available, so that the existence of a final equilibrium could not yet be adequately addressed. In particular, the conditions limiting the breach progression still represent a knowledge gap which cannot be solved using the knowledge on dam breaching. In fact, dam breaching is a headwater-dominated process, whereas the breaching of levee is dominated by both downstream boundary and backwater effects (Risher & Gibson, 2016). The breach growth can be limited by tailwater raising, inflow decreasing, topographic conditions, and breach repair operations (Nagy, 2006). Yet an equilibrium stage that is unconstrained by those factors has, to the authors' knowledge, never received a detailed attention. However, such an analysis is crucial to predict the consequences of the subsequent inundation and to manage the flood risk. For instance, from the Case 2 experiment by Kakinuma and Shimizu (2014), the water volume flooded during the final stable stage is about 70% of the total volume through the breach.

The aim of the present research is therefore to study the final stage of the breaching process and to formulate a new hypothesis for the existence of a final equilibrium. For this purpose, new laboratory experiments are

performed and the breaching process is monitored until an equilibrium between the breach and the hydraulic variables is likely reached under the nonlimiting conditions of steady inflow and without tailwater influence. Moreover, the experimental results are compared with those from literature and field data, and a first analysis of the final equilibrium is supported by an analytical flow model. Therefore, the present research contributes to improve the current knowledge about river levee breaching and meets the following research needs underlined by the ASCE-American Society of Civil Engineers / EWRI-Environmental & Water Resources Institute Task Committee on Dam/Levee Breaching (2011):

1. New laboratory experiments to better understand the complex processes of embankment breaching with a particular focus on the final stage;
2. Collection of data from real event case studies and from existing experiments; and
3. Proposition of a new theory for a final equilibrium of the river-breach system and formulation of a novel simplified hydraulic model.

2. Laboratory Experiments

2.1. Experimental Setup

The experiments were carried out in a 30-m long, 2-m wide, and 0.8-m-deep flume. The latter was subdivided longitudinally into the main channel, where the incoming discharge Q_u was set and the lateral channel used to evacuate the breach discharge Q_{br} (Figure 2).

A uniform sand (d_{10} = 0.64 mm, d_{50} = 0.84 mm, d_{60} = 0.88 mm, and $C_u = d_{60}/d_{10}$ = 1.375) was used both for the riverbed and the levee model. The levee section was trapezoidal (0.25-m high and 0.1-m wide at the crest with faces slope of 1V:2H), and the levee model was set longitudinally for a 15-m-long testing reach. A weight-tamping methodology was applied to 5-cm-thick layers of sand in order to compact the levee material and to avoid structural defects in the levee core. The goal of the experiments was to investigate the coupled processes of levee breaching and river hydromorphodynamics without reproducing real prototype conditions, so that the levee model should not be considered as an idealized scale model.

Toe drains were set at the levee base to control the seepage. The initial riverbed was flat, and the initial flow conditions were not able to induce sediment movement. A downstream sluice gate regulated the boundary condition in the main channel, and it was used to measure the downstream flow discharge Q_d.

The lateral channel was used to measure the breach discharge by means of a downstream sharp-crested weir, and backwater effects were avoided. This setup allowed the breach flow to be unrestrained, so that a final unconstrained equilibrium of the river-breach system could be investigated. More details on the laboratory experiments are given in Michelazzo and Oumeraci (2013).

2.2. Experimental Conditions and Measuring Techniques

The steady water inflow Q_u was the main test parameter, whereas no sediment discharge was inserted nor recirculated. For each value of Q_u = 10–70 l/s, the downstream sluice gate was set in order for the initial water level to be close to the levee crest and the initial flow was subcritical with Froude number F_0 = 0.02–0.23. The breach was triggered by overflow at the *breach trigger location* (BTL in Figure 2a), and the processes were captured by measuring water level, discharge and velocity, riverbed elevation, and breach evolution.

Three ultrasonic sensors (US0, US1, and US2 in Figure 2a) measured the water level in the main and lateral channels at the downstream sections and along the main channel. The inflow was measured by an electromagnetic flow meter; the seepage flow Q_{seep} was calculated using the model of Pavlovsky (1931), and the breach discharge $Q_{br,eq}$ at the equilibrium stage was determined as $Q_{br,eq} = Q_{lat} - Q_{seep}$, where Q_{lat} is the discharge of the lateral channel calculated using US2. The downstream discharge Q_d was calculated using the water level at US1, and the mass conservation was verified by considering the balance of the flow rates and the variation of the water storage. As a result, the breach outflow hydrograph Q_{br} (t) was calculated.

The 3-D components of the local flow velocity were measured by means of an acoustic doppler profiler. The riverbed in the main channel was surveyed at the beginning and at the end of each test by means of three submerged ultrasonic sensors, and a digital terrain model was generated. The evolution of the breaching process was recorded by two cameras, and the breach erosion rate and breach lengthening were obtained by video postprocessing.

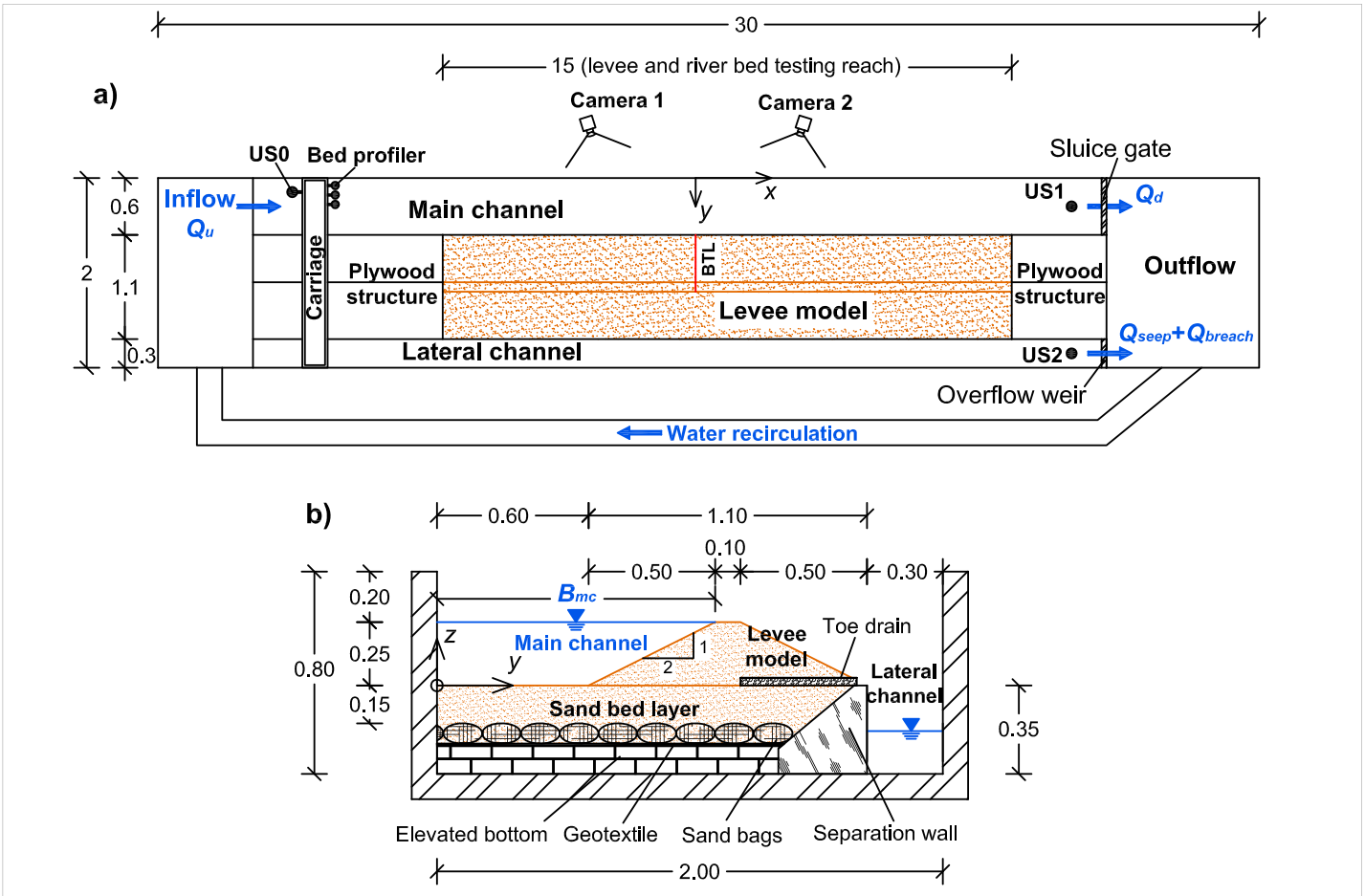

Figure 2. Experimental setup: (a) Plan view. (b) Cross section (dimensions in meters). BLT = breach trigger location.

To highlight the differences with the levee breach process, an additional test for the dam breach case was conducted with the downstream sluice gate being closed during the entire test duration t_{end}.

The experiments were performed according to three main testing phases:

1. Steady flow before breaching
2. Breach formation and evolution
3. Final equilibrium of the river-breach system

In the first testing phase, the downstream sluice gate was opened gradually and the inflow discharge was increased until the design inflow. The water level profile at the main channel centerline and the bed topography were measured during this steady phase.

In the second testing phase, a notch was cut on the levee crest at the BTL section, the breach was initiated by overflowing at the inception time $t_0 = 0$, and its formation and evolution were monitored. When the vertical erosion reached the bottom, the local toe drains that remained uncovered were removed in order to allow the erosion to fully develop vertically and to avoid partial obstructions. The drain system was constituted by independent parts, which could be removed independently from each other to avoid affecting the core of the intact portions of the levee.

In the third testing phase, the processes evolved until an equilibrium between the breach lengthening and the flow was achieved; the water level and levee crest profiles, the local flow velocities, and the main channel topography were then measured. Both steady and quasi steady conditions of the control variables breach length L_{br}, breach discharge Q_{br}, and water level Y_{US1} were examined in order to identify the equilibrium state. Conventionally, a control variable was considered in steady condition if its variation rate with respect

Table 1
Summary of Tests Performed and Main Results

Test name	Q_u (m^3/s)	t_{end} (min)	$r_{Q,eq}$ (−)	ε_{eq} (cm/s)	$L_{br,tot}$ (m)	$l_{br,dw}$ (%)	$t_{Qbr,max}$ (min)	$r_{Q,max}$ (−)	$t_{max,er}$ (min)	ε_{max} (cm/s)	$\Delta z_{b,max}$ (mm)
Dam breach	0	17.1	0	0.00	0.500	55%	3.4	1.00[a]	2.1	0.56	1.7
Q10	0.0101	146.9	0.674	0.00	1.050	67%	3.6	1.49	2.1	1.11	0.8
Q20	0.0201	150.7	0.496	0.00	1.050	79%	3.5	0.73	2.0	2.50	1.1
Q29	0.0292	222.2	0.470	0.00	1.450	86%	166.8	0.52	5.4	1.25	85.1
Q35	0.0353	119.5	0.433	0.00	1.525	82%	83.2	0.48	0.9	1.25	81.4
Q40	0.0404	115.4	0.397	0.01	1.724	85%	114.6	0.42	3.9	1.67	84.3
Q45	0.0451	86.8	0.457	0.01	1.874	85%	62.5	0.50	1.9	1.39	123.3
Q49	0.049	80.5	0.457	0.02	2.160	91%	73.7	0.48	3.4	1.39	93.9
Q55	0.0552	31.9	0.403	0.05	1.807	86%	29.6	0.44	1.2	1.50	125.8
Q60	0.0603	66.6	0.535	0.05	2.450	90%	47.9	0.64	1.6	1.88	121.0
Q70	0.0703	48.2	0.625	0.04	2.773	90%	43.9	0.67	3.1	1.25	140.9

[a]Calculated with respect to the maximum breach flow $Q_{br,max}$ = 0.0161 m^3/s.

to its mean value over the previous 5 min did not exceed the threshold of 1%; otherwise, the variations exceeding 1% were considered to be related to a quasi steady condition if they did not exceed about 5%. Tests with $Q_u \leq 40$ /s and $Q_u > 40$ l/s were found to be under steady and quasi steady conditions, respectively. Table 1 summarizes the main results in terms of discharge ratio $r_Q = Q_{br}/Q_u$ at the peak time $t_{Qbr,max}$ and at the equilibrium stage, total breach length $L_{br,tot}$ and its downstream percentage $l_{br,dw}$, maximum erosion rate ε_{max} of the breach length and its occurrence time $t_{max,er}$, erosion rate ε_{eq} at the equilibrium stage, and maximum bed deformation parameter $\Delta z_{b,max}$.

3. Results and Discussion

The experimental results are analyzed in terms of the temporal evolution and spatial configuration of the breach and flow characteristics. Tests Q29 and Q49 are chosen as typical cases of steady and quasi steady equilibrium states, respectively, and compared with the dam breach test.

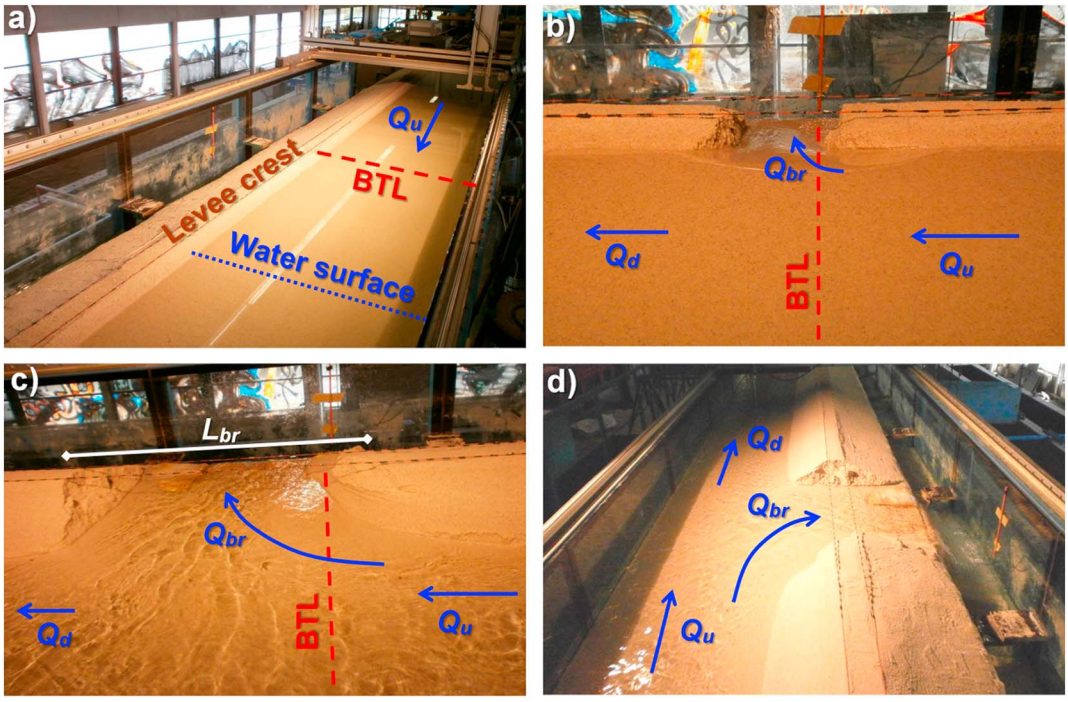

Figure 3. Sequence of photos during test Q29: (a) initial stage before breach triggering, (b) breach formation during stages 1–2, (c) breach evolution during stage 3, and (d) final equilibrium stage. BLT = breach trigger location.

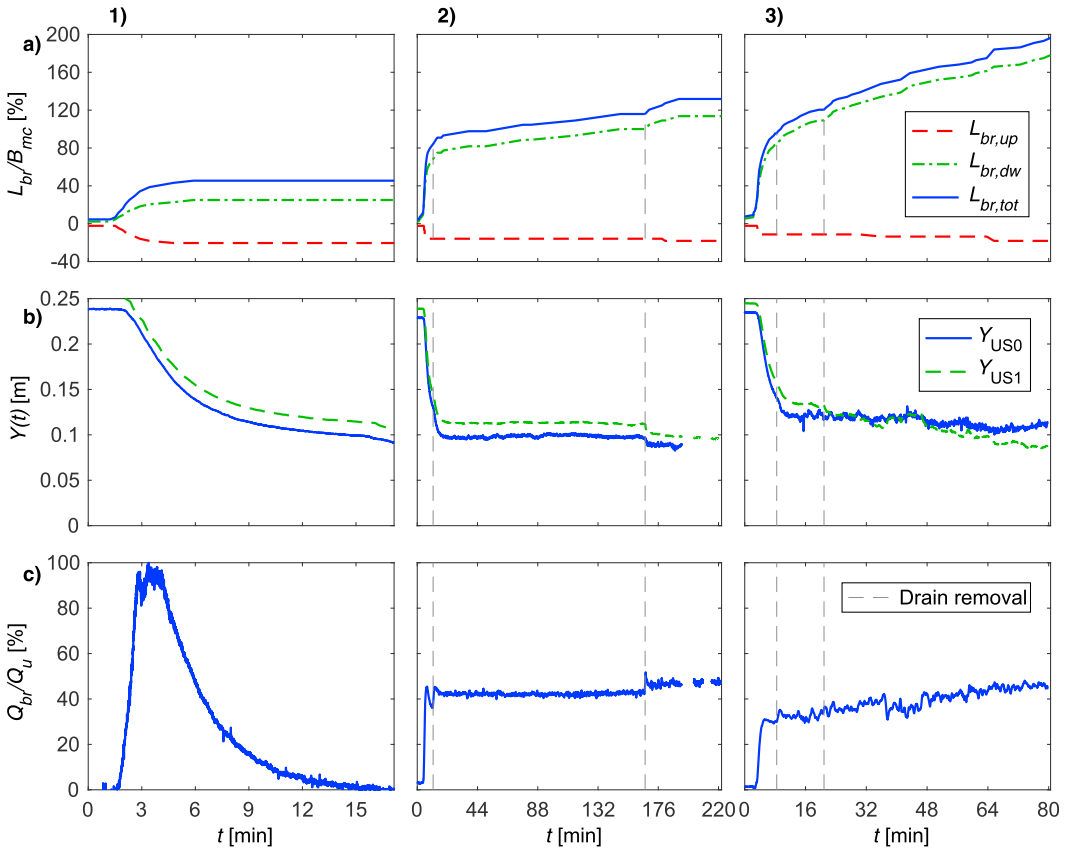

Figure 4. Time series of (a) dimensionless breach length, (b) water level in the main channel, and (c) dimensionless breach flow for (1) dam breach, (2) steady, and (3) quasi steady equilibrium tests. The maximum breach flow is used to compute the flow ratio of dam breach test (panel c1).

3.1. Breach Formation and Evolution

Several characteristics of the breaching process were found to be common from the initial stage before the breach triggering (Figure 3a) to the final stage of equilibrium (Figure 3d). Figures 3b and 3c highlight the breach downstream development with respect to the initial trigger line and the modification of the river flow field in terms of a slight disturbance (stages 1–2) to a more significant deflection (stage 3).

The temporal development of the dimensionless breach length L_{br}/B_{mc} (where B_{mc} = 1.1 m is the top width of the main channel associated to a water level at the levee crest, as indicated in Figure 2b) of the water level in the main channel and of the breach flow discharge ratio r_Q is reported in Figure 4 for the selected tests.

The overflow-induced erosion of the levee-protected side developed backward slowly during the initial stage, whereas the erosion rate increased when the levee crest was lowered (maximum erosion rate ε_{max} achieved at $t_{max,er} \approx$1–5 min) because the breach flow is strongly affected by the prevailing water level in the main channel. This creates a positive feedback to the breach development since the lower the levee crest, the larger is the lateral outflow which consequently has a stronger effect on the breach growth.

During the breach formation and the first breach evolution, that is, breaching stages 1–3 in Figure 1, the breaching mechanism consisted of a vertical erosion and a minor lateral erosion as a result of the combined effect of flow erosion processes and mass-wasting processes. The breach progressed mainly longitudinally after the breach channel reached the riverbed (stage 4 in Figure 1). Unlike the symmetrical development observed for the dam breach case, the levee breach lengthened asymmetrically with a prevalent downstream component while the upstream section remained almost stable, as also observed by Rifai et al. (2017). The ratio $l_{br,dw}$ of downstream breach length $L_{br,dw}$ at the equilibrium to total breach length $L_{br,tot}$ ranged between 67% and 91%, and larger values of the final breach length were generally achieved for larger inflow discharge.

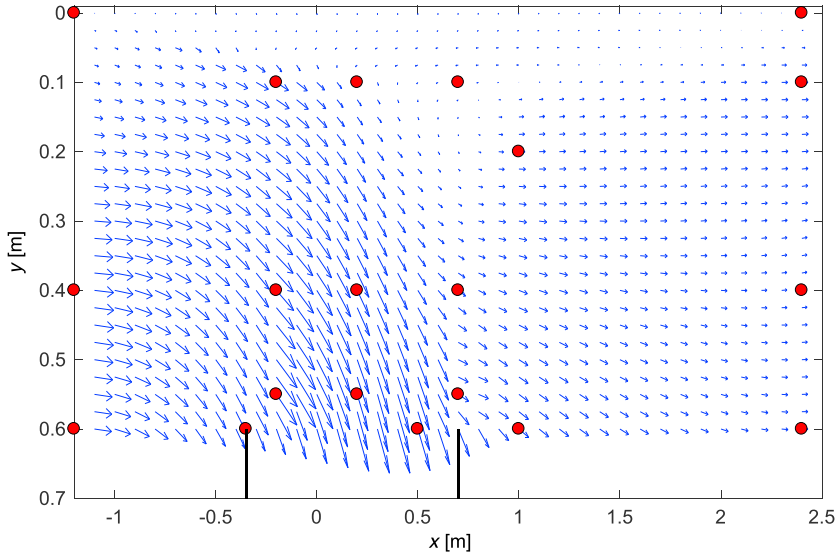

Figure 5. Depth-averaged flow field for test Q10 at the final stage. Actual measurement locations are indicated by circles and bold lines represent the breach upstream and downstream sections.

The breach lengthening progressed at smaller erosion rates during the successive breaching stages due to the lowering of the water level in front of the breach, and the erosion rate ε_{eq} at the final stage was 2 orders of magnitude smaller than ε_{max} (see Table 1). However, the breach channel reached a relatively stable length only for tests with $Q_u < 40$ l/s (Figure 4a2) and the final values of $L_{br,tot}$ were in the order of 1–2 times the width B_{mc}. Finally, the effect of the drain removal on the breaching process was to allow further vertical erosion and an increase of the outflow in the context of breach evolution toward the equilibrium stage.

The asymmetrical evolution of the breach length is due to the river flow deflection toward the breach (Figure 5), so that the transversal component of the flow velocity increases downstream, whereas the longitudinal component decreases as a result of the decreasing flow discharge in the river induced by the breach outflow. Moreover, a larger transversal component of the shear stress is expected downstream with the consequence of a larger erosive action. The experiments on zero-height side weirs conducted by Michelazzo et al. (2015) might help to detect the flow structures induced by the breach outflow in terms of (i) a *dividing surface zone* that distinguishes the streamlines through the breach from the other streamlines and (ii) a *flow separation zone* on the main channel side opposite to the breach, in which a streamline recirculation takes place.

3.2. Water Level and Flow Discharge

The hydraulic variables changed rapidly during the breaching process (Figures 4b and 4c). The upstream water level (US0) decreased due to the drawdown effect induced by the acceleration toward the breach. The downstream water depth (US1) decreased because the discharge diminished along the breach. Moreover, such behavior is consistent with the hydraulics of zero-height side weirs with increasing length (Michelazzo et al., 2015). The water level variation was small during the first stages, but it significantly changed when the levee section was eroded vertically. Finally, a steady or quasi steady water level Y was recorded as, respectively, depicted in Figures 4b2 and 4b3, with an equilibrium value in the order of 0.1 m. The equilibrium water level depends on both the boundary conditions and the breaching process that were different for each test according to the configuration set for the downstream sluice gate and the inflow.

The evolution of the discharge ratio $r_Q = Q_{br}/Q_u$ is analyzed in Figure 4c. The breach hydrograph was almost zero during the first breaching stage, but it increased rapidly during the second and third stages when the levee crest was lowered enough to make the process self-sustaining. Since the breach discharge depends on the water level at the breach, the lowering of the levee crest causes an increase of the overflow, and, as a consequence, a stronger erosive action takes place and the entire process itself increases. The breach discharge increased according to smaller gradients for larger breach lengths during the successive stages; it reached an equilibrium value that depends on the specific boundary conditions, as discussed by

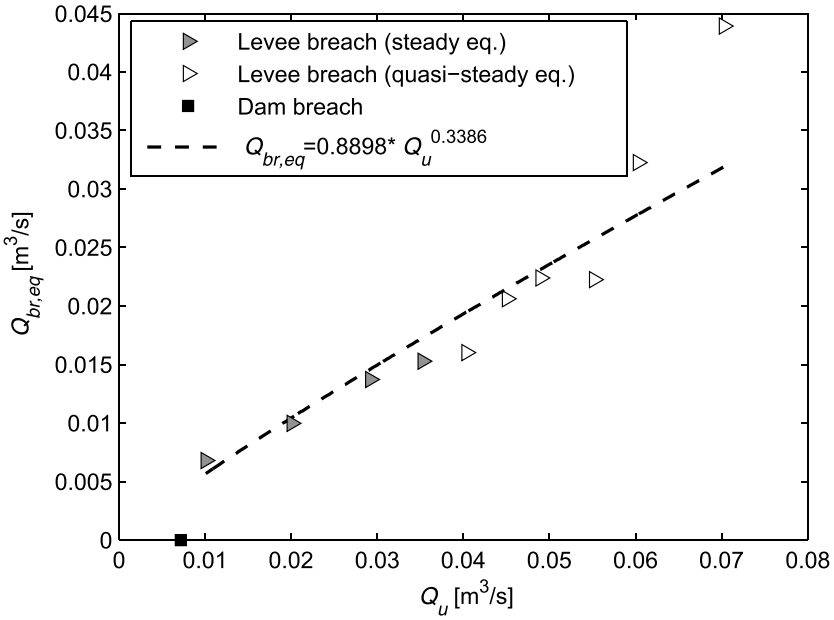

Figure 6. $Q_{br,eq}$ versus Q_u for each test and regression law.

Michelazzo et al. (2017) for the case of zero-height side weirs. Moreover, the final breach flow is strongly affected by the downstream boundary conditions and a larger breach flow is expected if a smaller downstream Froude number F_d is imposed, as in the case of a dead-end channel (Rifai et al., 2017).

The breach hydrograph reached a peak value (i.e., the first local maximum) after the first rapid increase during the third stage, but the absolute maximum occurred afterward at the time $t_{Qbr,max}$ for some tests. The breach flow changed toward a steady or quasi steady value during the fourth stage (Figures 4c2 and 4c3, respectively), and the effect of the drain removal was to induce some slightly larger equilibrium discharge value. The equilibrium breach discharge $Q_{br,eq}$ was smaller than the peak flow only for tests with $Q_u \leq 40$ l/s, whereas the breach flow increased after the local maximum for the other tests. A similar behavior was observed by Kakinuma and Shimizu (2014). This may be related to the combination between the rate of breaching progress and the flow field characteristics. It is realistic to expect the peak breach flow to be larger for faster development of the breach and for smaller initial Froude number F_0 (as in the limit case of dam break), whereas it will be less significant for low breach erosion rate and for larger F_0. However, several variables may affect the process, such as geotechnical properties of the levee material (grain size, compaction degree, levee cover layer, soil plasticity, etc.), geometrical and hydraulic conditions of the river, and morphology of the surrounding area.

A positive and significant correlation was found between steady inflow discharge Q_u and equilibrium breach flow discharge $Q_{br,eq}$ (Figure 6) for both steady and quasi steady equilibrium tests. In order to quantify the data correlation, a power law was selected as an appropriate regression model which could both explain the collected data and give realistic predictions in the extrapolation ranges. The model gives a good description of the collected data (R^2 = 0.91), and its significance is analyzed by means of F test, for which a confidence level of 95% was set and the correlation was found to be highly significant (P value <0.05).

3.3. Riverbed Modifications

The flow field disturbance induced by the breach outflow caused significant modifications to the riverbed. Erosion and deposition zones are clearly visible by analyzing the difference between the digital terrain models at the end (equilibrium phase) and at the beginning of the test (Figure 7a). Apart from the cases of dam breach and levee breach with low inflow ($Q_u \leq 20$ l/s), in which the bed deformations were not significant, a more evident morphology modification of the bed was found for the other tests. Erosion mechanisms and

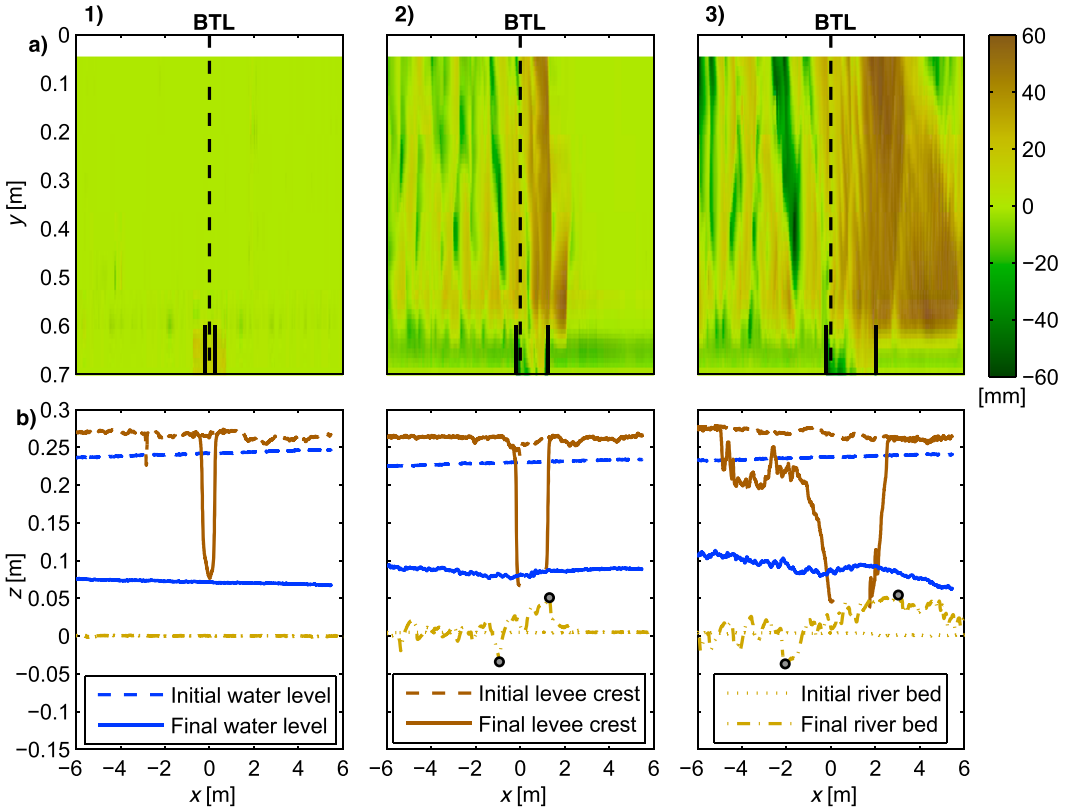

Figure 7. Spatial configuration of main and breach channel in terms of (a) difference of the digital terrain models between the final and the initial phases and (b) longitudinal profiles of levee crest, water level, and riverbed for (1) dam breach, (2) steady, and (3) quasi steady equilibrium tests. Solid vertical lines in panels a1–a3 depict the final breach channel. BLT = breach trigger location.

dunes developed upstream the BTL, whereas a deposition zone clearly developed downstream the BTL, and these trends were more pronounced for larger inflow.

The riverbed modifications are induced by the flow field (exemplary reported in Figure 5), and the effect of flow deviation toward the breach provides indications on the riverbed patterns. In particular, the upstream flow acceleration toward the breach channel was able to induce sediment motion; this mechanism was observed to be significant only for tests with $Q_u > 20$ l/s, for which the Shields parameter related to the mean upstream flow at the equilibrium was estimated to exceed the threshold of movement (assumed equal to 0.06). The erosion patterns were detected upstream, and the riverside slope of the levee was also affected. The material mobilized from the riverbed was conveyed out through the breach or deposited in the main channel along and downstream the breach due to flow deceleration. The deposition patterns developed according to the flow field in the zone located at the breach side and at the opposite side. Since the sediment is transported along the main flow streamlines, the deposition pattern was confined between the dividing surface zone and the flow separation zone with the tendency to develop along an oblique downward direction. The estimated Shields parameter at the downstream zone was under and over the incipient motion condition for tests with $20 < Q_u < 49$ l/s and $Q_u \geq 49$ l/s, respectively; this is confirmed by the extension of the downstream deposition.

The central longitudinal profiles of the levee crest (at $y = 1.15$ m), water level, and riverbed (at $y = 0.3$ m) are compared between initial and final stages in Figure 7b. The water level decreased along the entire main channel from the initial to the final stage, and the breach induced a drawdown profile upstream the breach and an increasing trend along the breach that is typical of a subcritical spatially varied flow.

Moreover, significant sediment transport processes were observed for tests with $Q_u \geq 29$ l/s, and the volume of both erosion and sedimentation increased with Q_u. The sediment transport processes induced a step-like riverbed feature in front and downstream of the breach; this feature was likely to induce a backwater profile

and to increase the breach outflow. A measure of the riverbed modification is analyzed by means of the maximum bed deformation parameter $\Delta z_{b,max}$, defined as the difference between the maximum and minimum bed elevations (gray circles in Figure 7b) in the vicinity of the breach along the main channel centerline. Except for the tests whose inflow was too small to induce sediment movement, parameter $\Delta z_{b,max}$ indicates that significant erosion and deposition occurred in almost every test and a positive correlation with the breach flow was found (Table 1).

3.4. Tentative Formulation of a New Hypothesis on the Existence of an Equilibrium Stage

The results obtained from the levee breach experiments seem to indicate the existence of a final equilibrium stage in the breaching process. The entire process evolves from the initial breach formation to the final equilibrium according to a transient phase which involves both river and breach characteristics. In particular, breach flow and water levels change rapidly during the first stages of the breach formation and then reach values that remain steady or quasi steady during the final stage, respectively, for tests with Q_u smaller or larger than 40 l/s (see Figure 4). The quasi steady variations of the control variables were larger for breach length L_{br} and downstream water level Y_{US1} than for breach flow discharge Q_{br}; this may be related to the following two key mechanisms:

1. A longer breach tends to increase the breach flow (positive feedback) which, however, is partially counterbalanced by the decrease of the downstream water level that affects the breach flow itself under subcritical flow conditions (negative feedback).
2. The effective breach channel, which conveys most of the breach flow, may represent only a portion of the total breach length. This is because the breach is eroded mainly downstream, whereas the upstream section is relatively stable, and some sand layers may also deposit at the upstream toe and obstruct the breach flow (as also observed by Rifai et al., 2017). Moreover, the breach flow distribution increases downstream due to the increase of transversal flow velocity and flow depth. As a result, the breach channel moves downstream and the consequent increase of the total breach length may not be related to a similar increase of the effective breach length. Finally, these effects were more pronounced for higher values of inflow discharge Q_u due to the larger longitudinal momentum in the main channel flow, which is also responsible of the residual lengthening of the breach.

Therefore, as a preliminary hypothesis for the equilibrium condition it is reasonable to assume that the hydraulic control of the breach is represented by the local headwater, which determines the flow through the breach and, as a consequence, the erosion rate. The local headwater is the result of the mutual interaction between breach flow and downstream river flow under subcritical conditions. As the breach flow increases and the breach lengthens, the local headwater decreases due to the reduction of the main flow and to the drawdown effect of the upstream water level, thus limiting a further increase of the breach flow.

Moreover, since the inflow is steady, the unsteadiness of the process originates from the riverbed and breach evolution which affects the flow characteristics. The larger breach flow induces a stronger erosive action so that sediment transport mechanisms take place with erosion/deposition upstream and downstream, respectively (see Figure 7); such bed modification affects the flow field itself. A larger erosion is exerted at the downstream breach section due to local flow deflection (Figure 5), and the downstream lengthening rate reduces when the breach outflow is distributed over a greater length. Finally, a residual breach erosion may be due to the effects of sediment transport mechanisms and to local two- and three-dimensional flow structures.

4. Comparison With Other Experimental Data and With Real Cases

The results of the levee breach experiments related to the existence of an equilibrium stage between the changes in flow characteristics and the breach evolution are relatively novel. Therefore, further published data and studies are analyzed, including both experiments and real events.

The collected data are summarized in Table 2, including geometrical and flow characteristics of main channel/river (e.g., upstream inflow Q_u, top width B_{mc} of the main channel/river associated to the water level, bed slope S_0, and reach morphology), the levee characteristics (e.g., height H_L and mean grain size d_{50}), breach trigger mechanism and breach characteristics (e.g., final length ratio $r_L = L_{br,tot}/B_{mc}$ and discharge

Water Resources Research

10.1029/2017WR021378

Table 2
Collection of Data From Experimental Studies (Exp) and Real Events (Riv) of Levee Breaches

Data set	Type and reference	Main channel morphology	B_{mc} (m)	Breach trigger	H_L (m)	d_{50} (mm)	Inflow condition	$Q_{u,eq}$ (m^3/s)	r_Q (−)	$F_{u,eq}$ (−)	$F_{d,eq}$ (−)	r_L (−)	Supposed limiting factors
ExpF&T	Experimental at laboratory scale (Fujita & Tamura, 1987)	Straight $S_0 = 0$	1.07	Overflow	0.100	0.64	Steady flow discharge	0.0158	0.633	0.403	0.148	0.654	HW
			1.07		0.080	0.64		0.0102	0.686	0.367	0.115	—	HW
			1.07		0.100	0.21		0.0095	0.632	0.242	0.089	0.336	HW
ExpISL	Experimental at laboratory scale (Islam, 2012)	Straight $S_0 = 0.1–0.2\%$	0.20	Overflow	0.150	1.00	Steady flow discharge	0.00895	0.894	0.451	0.048	3.500	—
			0.30		0.150	1.00		0.00871	0.941	0.607	0.036	2.167	—
			0.40		0.150	1.00		0.00869	0.932	0.788	0.054	3.525	—
			0.20		0.150	0.13		0.00949	0.843	0.478	0.075	3.550	—
			0.30		0.150	0.13		0.00885	0.893	0.617	0.066	2.767	—
			0.40		0.150	0.13		0.00493	0.832	0.704	0.119	2.088	—
ExpD&a	Experimental at laboratory scale (Dou et al., 2014)	180° curved bend $S_0 = 1\%$	0.60	Overflow	0.135	0.60	Steady flow discharge	0.01159	0.330	0.329	0.220	1.100	TW
			0.60		0.135	0.40		0.01157	0.349	0.328	0.213	1.217	TW
ExpK&S	Experimental at full scale (Kakinuma & Shimizu, 2014)	Straight $S_0 = 0.2\%$	14.00	Overflow	3.00	5.40	Flow hydrograph	35	0.714	0.495	0.141	2.143	—
			14.00		3.00	0.70		85	0.765	0.960	0.226	5.143	TW
ExpR&a	Experimental at laboratory scale (Rifai et al., 2017)	Straight $S_0 = 0$	1	Overflow	0.3	1	Steady flow discharge	0.02	0.987	1.023	0.013	1.960	HW
			1		0.3	1		0.021	0.985	0.980	0.015	1.990	HW
			1		0.3	1		0.028	0.979	0.964	0.020	2.260	HW
			1		0.3	1		0.03	0.965	0.996	0.035	2.240	HW
			1		0.3	1		0.031	0.967	1.010	0.033	2.230	HW
RivVer	Versilia river event (Preti et al., 1996)	90° curved bend $S_0 = 0.1\%$	60	Overflow	5	—	Flow hydrograph	447.24	0.675	0.482	0.157	1.133	HW
RivMus	Muson dè Sassi river event (Viero et al., 2013)	Straight	14	Piping	5	0.1	Flow hydrograph	39.71	0.580	0.258	0.110	1.429	HW + TW
RivOmb	Ombrone Pistoiese event (Physis Ltd, 2010)	Straight $S_0 = 0.05\%$	21	Piping	4	—	Flow hydrograph	187.593	0.386	0.268	0.160	0.952	HW + TW
RivSer	Serchio river event (Bonanni et al., 2010; CFRT-Hydrometeorological center of Tuscany region and ADBS-River basin authority of river Serchio, 2010)	Straight $S_0 = 0.04\%$	190	Piping	6	—	Flow hydrograph	1800	0.611	0.504	0.196	0.842	HW + TW
RivBac	Bacchiglione river event (Viero et al., 2012, 2013)	Straight	28	Piping	6	0.1	Flow hydrograph	593.36	0.360	0.246	0.158	1.415	BR
RivSec	Secchia river event (Orlandini et al., 2015)	Straight	50	Animal burrows and piping	6	—	Flow hydrograph	390	0.821	0.894	0.138	1.600	—

Note. HW = headwater; TW = tailwater; BR = breach repair.

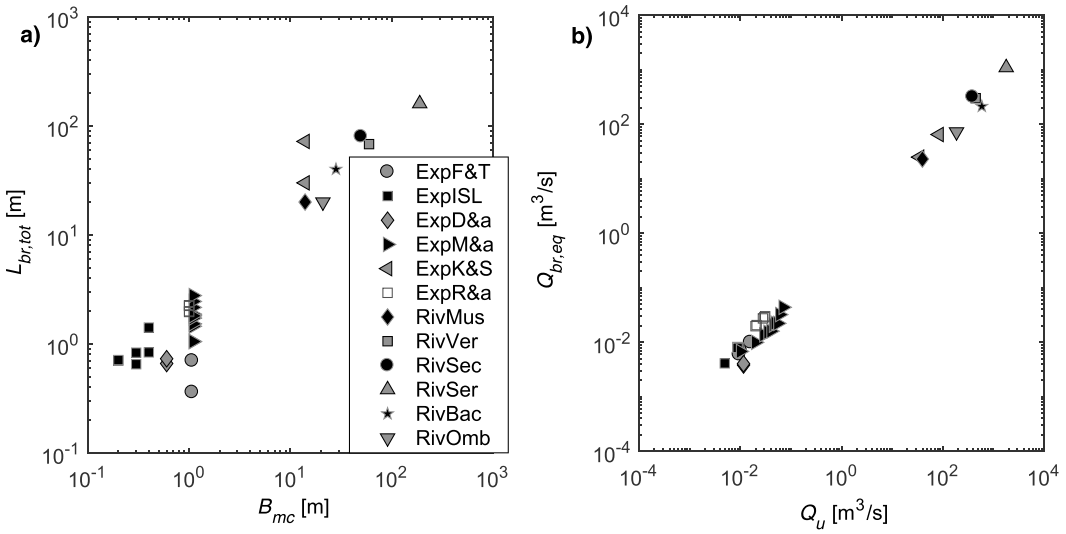

Figure 8. Breach characteristics in comparison with river variables in terms of (a) total breach length and (b) equilibrium flow rate. Present study data are indicated as *ExpM&a*.

ratio $r_Q = Q_{br,eq}/Q_u$). The occurrence of an equilibrium stage is detected on the basis of the results of the data analysis. Moreover, a hypothesis for the conditions limiting the breaching process is proposed based on the following three possible cases or their combinations:

1. *Tailwater* (*TW*): the breaching process is limited by the tailwater raising on the protected side that balances the headwater.
2. *Headwater* (*HW*): the breaching process is limited by the headwater decreasing due to inflow diminishing.
3. *Breach repair* (*BR*): the breaching process is limited by breach repair operations.

In particular, the collected data are from 18 experimental tests of five research studies and from six real events, ranging from laboratory experiments to full scale observations. The breaching processes for the collected data differ in terms of levee material and geometry, river flow and morphology, topography of riverbed and protected land, breach trigger mechanism, and time and spatial scales of the processes. The data were elaborated in order to get the relevant information for the present study by analyzing the references and through personal communications and support by the authors for the Muson dei Sassi, Ombrone Pistoiese, Serchio, and Bacchiglione rivers and for the laboratory study of Rifai et al. (2017).

Data sets were selected only if signs of a trend toward stability could be recognized in terms of steady or quasi steady conditions of water level, flow rates, or breach length. Such an equilibrium state may be detected at the end of the tests for the experimental works, since a steady inflow or an inflow hydrograph with small variations during the last stage was used. In particular, only those tests clearly exhibiting stability were selected from the experimental data of Fujita and Tamura (1987), Kakinuma and Shimizu (2014), and Rifai et al. (2017). On the other hand, the equilibrium for the real events may be identified at the time intervals of the flow hydrograph during which a steady or a quasi steady state occurred in terms of both breach flow Q_{br} and river flow Q_u (for events of Ombrone Pistoiese, Serchio, and Secchia rivers) or at least in terms of their ratio $r_Q = Q_{br}/Q_u$ (for events of Versilia, Muson dè Sassi, and Bacchiglione rivers). Such conditions were found at the passage of the river peak hydrograph, during which the hydraulic variables varied slightly for time intervals in the order of some hours.

The geometrical and flow characteristics of the levee breaches are plotted in Figure 8 as a function of the main channel variables.

A data scatter is observed regarding the final breach length (Figure 8a) which reflects the dependence of this parameter on multiple factors. The geotechnical properties of the levee definitely play a key role for the breaching dynamics and the erosion rate, which depends on the material resistance. Also, the dimensions and the geometry of the levee can influence the development of the breach and its lengthening. Moreover, the morphology of the river reach (straight, curved, etc.) generates local hydraulic conditions. The topographic conditions on the protected side may also affect the outflow process if backwater effects

take place and reduce the breach flow. The breach trigger mechanism may also affect the final breach length, even if its effect on river levee breaching has not been investigated unlike for the dam-breach cases (Froehlich, 2008), and flood emergency countermeasures may limit the breach development.

On the other hand, the equilibrium breach flow is strongly correlated to the inflow (Figure 8b) both for the laboratory and the real event scale, for which the discharge varies within 5 orders of magnitude. It is likely that the breach length is a more sensitive parameter to the multiple factors affecting the process than the breach discharge and that a kind of equilibrium is reached faster for water flow than for sediment transport, as observed in the movable bed experiments of the present study.

5. Analytical Model for Breach Flow Evolution Toward a Final Equilibrium Stage

The breach evolution is analyzed herein solely from the perspective of the river hydraulic processes. Since the breach outflow process resembles a side weir flow (Kamrath et al., 2006; Oertel et al., 2011; Saucier et al., 2009), it is considered here that, once the levee breach has reached the riverbed, the breach channel may be modeled as a zero-height side weir that lengthens during a time sequence of steady states. Michelazzo (2015) simulated the subcritical steady flow through a zero-height side weir by means of a specific model that is used here to provide a hydraulic interpretation of the breaching process at the final equilibrium stage.

The model solves the energy and mass conservation equations according to the De Marchi's approach (1934), and the solution is given in terms of dimensionless ratios of the flow and geometrical variables as functions of the Froude numbers at the upstream (F_u) and downstream (F_d) cross sections of the breach (further details in Michelazzo, 2015):

$$\text{Flow discharge ratio } r_Q = \frac{Q_{br}}{Q_u} = 1 - \frac{F_d}{F_u} \cdot \left(\frac{2 + {F_u}^2}{2 + {F_d}^2} \right)^{3/2} \tag{1}$$

$$\text{Length ratio } r_L = \frac{L_{br}}{B} = \frac{\Phi(F_d) - \Phi(F_u)}{C_d} \tag{2}$$

where $\Phi(F) = F\sqrt{2} - 3\sin^{-1}\left(F\sqrt{\frac{1}{2+F^2}}\right)$, B is the main channel width, and C_d is the discharge coefficient here formulated with a modification of that proposed by Michelazzo et al. (2017) for the case of zero-height side weirs with a correction coefficient equal to 0.55:

$$C_d = 0.256 - 0.103 \cdot F_u - 0.072 \cdot F_d - 0.022 \cdot r_L \tag{3}$$

It should be noted that the combination of equations (2) and (3) may result in two solutions for the length ratio r_L, but only one is physically consistent with the hydraulics of a side weir as described by the model of Michelazzo (2015). Moreover, the outflow process is described as a disturbance induced to the main channel flow field which modifies the Froude number from upstream to downstream. A lengthening of the levee breach induces a larger outflow and greater acceleration in the upstream section that results in an increase of F_u, whereas the downstream flow is less affected by the outflow and mainly governed by the downstream boundary condition, at least in the subcritical regime. The breaching process is represented as patterns of the breach ratios r_Q and r_L as functions of F_d and F_u, which develop from the initial undisturbed flow condition ($F_d = F_u$ when no outflow occurs) toward a final stage ($F_u > F_d$ for subcritical flow) as determined by equations (1)–(3). According to the assumption of the model, the flow pattern should be considered as a succession of steady states, whereas transient variations are not captured by the model.

The analytical model is applied to the data presented in Section 4 in order to predict the flow discharge ratio r_Q and the length ratio r_L. A realistic prediction is obtained for r_Q with 85% of data predicted within a ± 10% error range (Figure 9b). A worse prediction of the water discharge ratio r_Q is obtained for those tests of the present study which did not reach a steady equilibrium.

In contrast, a larger scatter is obtained for r_L with 73% of data predicted within a ± 50% error range (Figure 9a). Some real events and other experimental data are affected by significant prediction errors regarding the length ratio r_L. Moreover, the breach length prediction is affected by the uncertainty on the discharge coefficient formulation, together with other flow, morphological, geometrical, and geotechnical factors, and by limitations of the analytical model to represent the high complexity of the real processes. In particular, the breach erosion may not develop vertically until the riverbed, likely resulting in an underestimation of the

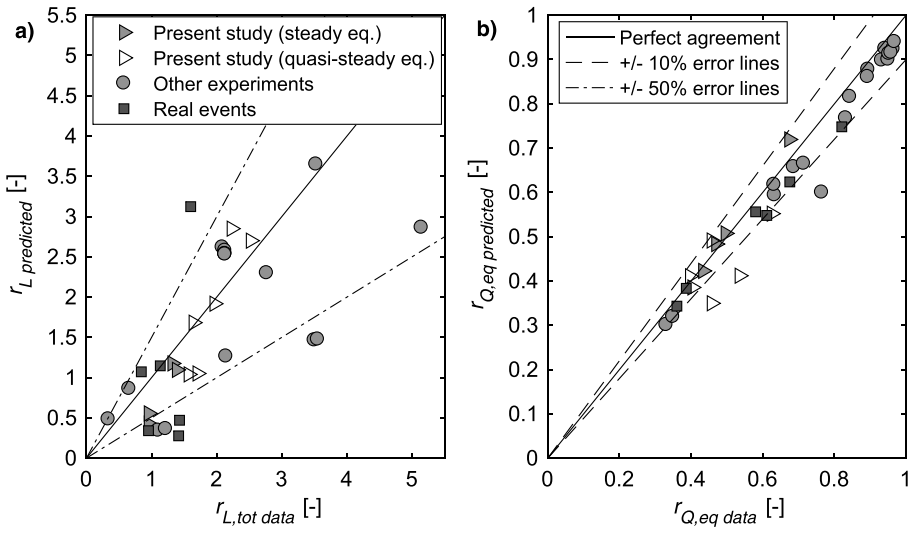

Figure 9. Model prediction in terms of (a) length ratio r_L and (b) water discharge ratio r_Q.

length ratio because a lower breach needs a smaller length to convey the breach flow. In general, the breach morphology differs from the rectangular shape assumed by the model, since the breach channel sides are not vertical and the breach shape is three-dimensional. Moreover, the flow is assumed as one-dimensional whereas three-dimensional zones develop during the breaching process. All these issues add uncertainty in the prediction of the breach characteristics by the model, which cannot represent the complex transient hydromorphodynamic and geotechnical processes of the real phenomenon.

Nevertheless, the analytical model provides a new insight into the river hydrodynamics during the breaching process until the final stage as well as indications for a possible straightforward prediction of the main breach characteristics.

Finally, an approach to provide the theoretical upper envelope of the breach characteristics is proposed by assuming that the breach develops vertically until the riverbed is reached and longitudinally until the critical flow occurs in the upstream section ($F_u = 1$). The downstream flow regime is governed by the specific boundary condition, so that the upper envelopes $r_{Q,env}$ and $r_{L,env}$ of the flow and length ratios, respectively, are obtained from equations (1)–(3):

$$r_{Q,env} = 1 - F_d\left(\frac{3}{2+{F_d}^2}\right)^{3/2} \tag{4}$$

$$r_{L,env} = \frac{F_d\sqrt{2} - 3\sin^{-1}\left(F_d\sqrt{\frac{1}{2+{F_d}^2}}\right) + 0.432}{C_{d,env}} \tag{5}$$

$$C_{d,env} = 0.153 - 0.072{\cdot}F_d - 0.022{\cdot}r_{L,env} \tag{6}$$

The upper envelope curves of the breach length ratio $r_{L,env}$ and the breach flow discharge ratio $r_{Q,env}$ as functions of downstream Froude number F_d calculated by equations (4)–(6) are plotted in Figure 10 together with the data collected in section 4. The theoretical curves represent indeed an upper limit for most of the data, and the decreasing trend of r_Q with F_d is confirmed. The amount of data exceeding the theoretical curves is larger for breach flow discharge ratio r_Q (Figure 10b) than for breach length r_L (Figure 10a). However, the mean difference between the data exceeding the upper envelope $r_{Q,env}$ and the theoretical values given by equation (4) is 7%, with 67% of these data having differences smaller than 5%. This represents a relatively good result given all the uncertainties associated with the flow and geometrical parameters, the model's limitations, and the complexity of the physical processes. Equations (4)–(6) provide a first approximation of the order of magnitude that the breach variables may reach during the last stage of the breaching process.

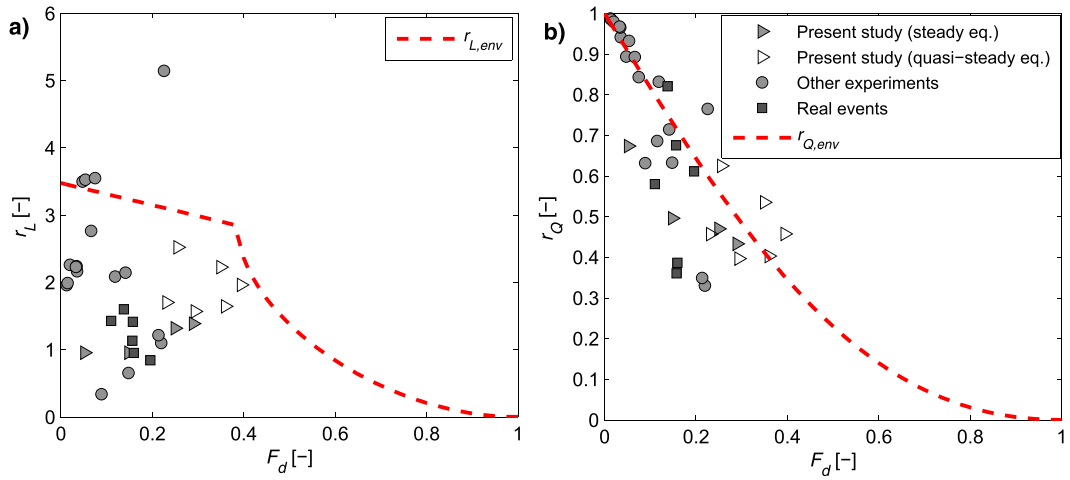

Figure 10. Envelope curves of (a) breach length ratio r_L and (b) breach flow discharge ratio r_Q and comparison with experimental and field data.

Therefore, they represent a straightforward tool to predict the breaching consequences, which might be useful for real-time and long-term analyses in river basin systems and for flood risk studies.

6. Summary and Concluding Remarks

A new laboratory study was conducted at a relatively large scale in order to investigate the hydromorphodynamic processes that govern the breaching of an earthen river levee made of noncohesive material. The experimental investigations reproduced the overflow-induced breaching for a river levee. The breach formation and evolution were monitored by recording flow depth, discharge and velocity, breach length, and riverbed. Unlike previous levee breaching studies, the present experiments focus on the evolution of both breach and river variables as well as on the attempt to identify and examine an equilibrium state of the river-breach system during the last stage of the breaching process.

The breach evolution process was described, and an explanation for the mainly downstream development of the breach was introduced and supported by the analysis of the flow field. Flow discharge, velocity, and depth were analyzed, and the effect of the breach outflow on the processes related to sediment transport and riverbed modifications was also highlighted. Based on the performed experiments and analyses, a new hypothesis about the existence of such an equilibrium state was tentatively proposed in terms of a balance between breach flow and upstream river flow, even if the breach length may still develop according to a residual erosion rate.

The results of the present study, which provides a significant set of new data and their analysis, were compared with other laboratory experiments and real cases. The main characteristics of the breaching process were summarized, and the breach characteristics were compared with the river characteristics in order to further analyze the equilibrium stage.

The breach flow was described within the framework of an analytical hydrodynamic model that solves the governing equations of a subcritical zero-height side weir with the boundary conditions expressed as Froude numbers. A new description of the breach outflow was then proposed, and all the collected data were used to test the model at the equilibrium stage. As a result, a satisfactory prediction was achieved regarding the breach flow discharge ratio, whereas the breach length ratio was affected by a larger scatter. The latter may be due to the uncertainty in the discharge coefficient and many other flow and geotechnical factors as well as to the limitations of the analytical model. Moreover, the model was reformulated in terms of the upper envelopes of the breach length ratio $r_{L,env}$ and the breach discharge ratio $r_{Q,env}$ that might be useful for flood risk mitigation and management purposes.

The results of the present research are intended to provide an improved insight into the mechanisms underlying the evolution of the river-breach system, particularly from the perspective of the hydraulic processes.

Though the results cannot be directly scaled up to a real levee, the findings were compared with real events data and a relatively good agreement has been found in the prediction of the breach length ratio and the flow discharge ratio. Therefore, the results are encouraging for further research and the proposed formulae may provide a first approximation regarding the equilibrium of real levee breaches. An improved knowledge of the entire breaching process and the river-breach system is crucial for flood risk management as it might support the analysis of the flood risk zones (in terms of flood depth, velocity, and arrival time) for alerting operations and provide useful indications for breach emergency repair operations.

Notation

The following main symbols are used in this paper:

B_{mc}	= top width of the main channel/river associated to the water level	(m)
C_d	= discharge coefficient	(−)
d_{50}	= mean grain size	(mm)
F_0	= initial Froude number	(−)
F_d	= downstream Froude number	(−)
F_u	= upstream Froude number	(−)
H_L	= levee height	(m)
L_{br}	= breach length	(m)
$L_{br,dw}$	= downstream component of breach length	(m)
$L_{br,up}$	= upstream component of breach length	(m)
$L_{br,tot}$	= total breach length	(m)
Q_{br}	= water discharge flowing in the breach	(m^3/s)
Q_d	= water discharge flowing downstream	(m^3/s)
Q_{lat}	= water discharge in the lateral channel	(m^3/s)
Q_{seep}	= seepage flow through the levee toe drains	(m^3/s)
Q_u	= water discharge flowing upstream	(m^3/s)
r_L	= length ratio	(−)
r_Q	= water discharge ratio	(−)
S_0	= riverbed or flume slope	(−)
t	= time coordinate	(s)
Y	= water level	(m)

Greek symbols:

ε	= erosion rate of breach length	(m/s)
$\Delta z_{b,max}$	= maximum bed deformation parameter	(m)

The subscripts associated to a variable are referred to the following:

- 0 = before breaching stage;
- *br* = breach channel;
- *d* = zone located downstream of the breach;
- *eq* = equilibrium stage in the breaching process;
- *u* = zone located upstream of the breach;
- *x* = longitudinal direction;
- *y* = transverse direction;
- *z* = vertical direction.

Acknowledgments
The laboratory investigations presented in this paper were carried out in the facility of the Hydraulic Engineering Division of the Leichtweiß-Institute for Hydraulic Engineering and Water Resources of the Technical University of Braunschweig, Germany (LWI). They were supported and supervised by the Hydromechanics and Coastal Engineering Division of the LWI within the framework of a PhD research project, whose details are reported comprehensively in Michelazzo and Oumeraci (2013) and more concisely in Michelazzo (2014). Moreover, data sets used for Figures 4, 5, and 7 are provided in the supporting information. Data presented in section 4 regarding other studies and real events are from cited references. In particular, Viero, D. P. is acknowledged for the support and the data provided regarding the levee breach events of Muson dei Sassi and Bacchiglione rivers. Sadun, S. and Settesoldi, D. are acknowledged for the support given to analyze the levee breaches of Serchio and Ombrone Pistoiese rivers, respectively. Rifai, I. is acknowledged for the support and the data provided regarding the experiments by Rifai et al. (2017).

References

ASCE-American Society of Civil Engineers/EWRI-Environmental & Water Resources Institute Task Committee on Dam/Levee Breaching (2011). Earthen embankment breaching. *Journal of Hydraulic Engineering*, *137*(12), 1549–1564. https://doi.org/10.1061/(ASCE)HY.1943-7900.0000498

Bhattarai, P. K., Nakagawa, H., Kawaike, K., & Zhang, H. (2015). Analysis of breach characteristics and equilibrium scour pattern for overtopping induced river dyke breach, Annual of Disas. Prev. Res. Inst., Kyoto Univ., N. 58 B.

Bonanni, G., Carli, A., Casarosa, N., Ceragioli, M., Dell'Aiuto, S., Della Maggesa, M., et al. (2010). The levee breach of river Serchio at Malaventre (Nodica) during 25 December 2009, Il Geologo (in Italian). *Italian Journal of Geologists*, *21*(79).

CFRT-Hydrometeorological center of Tuscany region, & ADBS-River basin authority of river Serchio (2010). Report on the flooding event of river Serchio during 24–25 December 2009, (in Italian). Retrieved from http://www.cfr.toscana.it/supports/download/eventi/report_evento_alluvionale_serchio_2009-12-25.pdf

Chen, Y. Z., Syvitski, J. P. M., Gao, S., Overeem, I., & Kettner, A. J. (2012). Socio-economic impacts on flooding: A 4000-year history of the Yellow River, China. *Ambio*, *41*(7), 682–698. https://doi.org/10.1007/s13280-012-0290-5

Construction Industry Research and Information Association, Ministry of Ecology, and USACE-United States Army Corps of Engineers (2013). *The international levee handbook*. London: CIRIA.

De Marchi, G. (1934). Theoretical knowledge on the functioning of side weirs (in Italian). *L'Energia Elettrica*, *11*(11), 849–860.

Dou, S. T., Wang, D. W., Yu, M. H., & Liang, Y. J. (2014). Numerical modeling of the lateral widening of levee breach by overtopping in a flume with 180° bend. *Natural Hazards and Earth System Sciences*, *14*(1), 11–20. https://doi.org/10.5194/nhess-14-11-2014

Froehlich, D. (2008). Embankment dam breach parameters and their uncertainties. *Journal of Hydraulic Engineering*, *134*(12), 1708–1721. https://doi.org/10.1061/(ASCE)0733-9429(2008)134:12(1708)

Fujita, Y., & Tamura, T. (1987). Enlargement of breaches in flood levees on alluvial plains. *Journal of Natural Disaster Science*, *9*(1), 37–60.

Govi, M., & Maraga, F. (2005). Inundation on the Po Plain caused by levee breaches. *Giornale di Geologia Applicata*, *1*, 167–176. Retrieved from http://www.aigaa.org/AIGA/public/GGA.2005-01.0-17.0017.pdf

Islam, M. S. (2012). Study on levee breach and successive disasters in low-land through numerical and experimental approaches (PhD dissertation). Japan: Nagoya University. Retrieved from http://hdl.handle.net/2237/17336

Islam, M. S., & Tsujimoto, T. (2011). Characteristics of flood disasters in low floodplain along a big river due to overflow levee breach. *International Journal of GEOMATE*, *1*(1), 52–63.

Islam, M. S., & Tsujimoto, T. (2015). Experimental and numerical approaches to overtopping levee breach effects in a river and floodplain, Amer. *Journal of Civil Engineering*, *3*(2), 31–42. https://doi.org/10.11648/j.ajce.20150302.12

Kakinuma, T., & Shimizu, Y. (2014). Large-scale experiment and numerical modeling of a riverine levee breach. *Journal of Hydraulic Engineering*, *140*(9), 04014039. https://doi.org/10.1061/(ASCE)HY.1943-7900.0000902

Kamrath, P., Disse, M., Hammer, M., & Koengeter, J. (2006). Assessment of discharge through a dike breach and simulation of flood wave propagation. *Natural Hazards*, *38*(1–2), 63–78. https://doi.org/10.1007/s11069-005-8600-x

Michelazzo, G. (2014). River levee breaching: Analytical flow modelling and experimental hydro-morphodynamic investigations, (PhD dissertation). TU Braunschweig and Florence University. Retrieved from http://digisrv-1.biblio.etc.tu-bs.de:8080/docportal/servlets/MCRFileNodeServlet/DocPortal_derivate_00035018/2014_Michelazzo_Dissertation.pdf

Michelazzo, G. (2015). New analytical formulation of De Marchi's model for a zero-height side weir. *Journal of Hydraulic Engineering*, *141*(12), 04015030. https://doi.org/10.1061/(ASCE)HY.1943-7900.0001047

Michelazzo, G., & Oumeraci, H. (2013). River levee breaching—Mobile bed laboratory investigations (LWI Report N. 1039, 129 pp.).

Michelazzo, G., Oumeraci, H., & Paris, E. (2015). Laboratory study on 3D flow structures induced by zero-height side weir and implications for 1D modelling. *Journal of Hydraulic Engineering*, *141*(10), 0401502. https://doi.org/10.1061/(ASCE)HY.1943-7900.0001027

Michelazzo, G., Oumeraci, H., & Paris, E. (2017). Closure to "Laboratory study on 3D flow structures induced by zero-height side weir and implications for 1D modelling" by Giovanni Michelazzo, Hocine Oumeraci, and Enio Paris. *Journal of Hydraulic Engineering*, *143*(3), 07016011. https://doi.org/10.1061/(ASCE)HY.1943-7900.0001257

Nagy, L. (2006). Estimating dike breach length from historical data. *Periodica Polytechnica Serial Civil Engineering*, *50*(2), 125–139.

Oertel, M., Carvalho, R. F., & Jansen, R. H. A. (2011). Flow over a rectangular side weir in an open channel and resulting discharge coefficients, Proc. of the 34th World Congress of the International Association for Hydro- Environment Research and Engineering: 33rd Hydrology and Water Resources Symposium and 10th Conference on Hydraulics in Water Engineering, Brisbane, Australia.

Orlandini, S., Moretti, G., & Albertson, J. D. (2015). Evidence of an emerging levee failure mechanism causing disastrous floods in Italy. *Water Resources Research*, *51*, 7995–8011. https://doi.org/10.1002/2015WR017426

Pavlovsky, N. N. (1931). Seepage through earth dam, Insit. Gidrotekhniki I Melioratsii. Leningrad, (in German), translated by U.S. Corps of Engineers, Vicksburg, Miss.

Physis Ltd (2010). Technical consultant regarding the flooding events of 23–25 December 2009 (in Italian).

Preti, F., Paris, E., & Settesoldi, D. (1996). Flooding event of 19 June 1996 in Versilia-Garfagnana Area: Analysis of flood hydrographs, Proc. Conference "La difesa dalle alluvioni", Florence (Italy) 4-5/11/1996, 341–354 (in Italian).

Rifai, I., Erpicum, S., Archambeau, P., Violeau, D., Pirotton, M., El Kadi Abderrezzak, K., & Dewals, B. (2017). Overtopping induced failure of noncohesive, homogeneous fluvial dikes. *Water Resources Research*, *53*, 3373–3386. https://doi.org/10.1002/2016WR020053

Risher, P., Gibson, S., & Gibson, S. (2016). Applying mechanistic dam breach models to historic levee breaches, FLOODrisk 2016-3rd European Conference on Flood Risk Management, Lyon, France. https://doi.org/10.1051/e3sconf/20160703002

Saucier, C. L., Howard, I. L., & Tom, J. G. (2009). Levee breach geometries and algorithms to simulate breach closure, SERRI Report 70015–001, U.S. Department of Homeland Security, Science and Technology Directorate Washington, DC 20528.

Sills, G. L., Vroman, N. D., Wahl, R. E., & Schwanz, N. T. (2008). Overview of New Orleans levee failures: Lessons learned and their impact on national levee design and assessment. *Journal of Geotechnical and Geoenvironmental Engineering*, *134*(5), 556–565. https://doi.org/10.1061/(ASCE)1090-0241(2008)134:5(556)

Viero D. P., D'Alpaos, A., Carniello, L., & Defina, A. (2012). A coupled hydrodynamic model for river levee breach simulation, Proc. of XXXIII Italian Meet. of Hydr. and Hydr. Constr., Brescia (Italy), 10–15 September 2012 (in Italian).

Viero, D. P., D'Alpaos, A., Carniello, L., & Defina, A. (2013). Mathematical modeling of flooding due to river bank failure. *Advances in Water Resources*, *59*, 82–94. https://doi.org/10.1016/j.advwatres.2013.05.011

Vorogushyn, S., Merz, B., Lindenschmidt, K. E., & Apel, H. (2010). A new methodology for flood hazard assessment considering dike breaches. *Water Resources Research*, *46*, W08541. https://doi.org/10.1029/2009WR008475